Materials Today Sustainability 19 (2022) 100186

Contents lists available at ScienceDirect

Materials Today Sustainability

journal homepage: https://www.journals.elsevier.com/materials-today-sustainability

Improved mechanical and microstructural performance of high-density polyethylene–chitosan–hydroxyapatite composites as potential bone implant materials

M. Shelly [a], M. Raghavendra [b], A. Prabhu [c], H.B. Ravikumar [b], M. Mathew [d], T. Francis [a, *]

[a] Department of Chemistry, St. Joseph's College (Autonomous), Devagiri, Calicut, Kerala, 673008, India
[b] Department of Studies in Physics, University of Mysore, Manasagangotri, Mysuru, Karnataka, 570006, India
[c] Yenepoya Research Centre, Yenepoya University, Mangalore, Karnataka, 575018, India
[d] Department of Physics, St. Joseph's College (Autonomous), Devagiri, Calicut, Kerala, 673008, India

ARTICLE INFO

Article history:
Received 29 March 2022
Received in revised form
12 June 2022
Accepted 25 June 2022
Available online 1 July 2022

Keywords:
Biocomposite
Biocompatibility
Free hole volume
MC3T3-E1 cell lines
Thermal stability

ABSTRACT

High-density polyethylene (HDPE)–chitosan–hydroxyapatite hybrid composite series with varying concentration of hydroxyapatite were prepared and compared with its corresponding HDPE-chitosan binary composite. The microstructural and mechanical characterizations of the prepared composites were studied. A 12% increase for the composite system with 8 wt% hydroxyapatite (HA4) has been noted when compared with its corresponding binary system and has been optimized for further applications. The structural characterization and miscibility of the components in the composite system were studied by using Fourier transform infrared spectroscopy and X-ray diffractometry. Positron annihilation lifetime spectroscopy studies showed that the free holes are formed in the range of ~115.8 $Å^3$. Contact angle studies and sorption studies were further correlated with the biocompatibility analysis to study cell adhesion and protein absorption on the surface of the composites. MC3T3 E1 cell lines showed good cell proliferation on the optimized systems. The presence of micropores along with chitosan and hydroxyapatite promoted cell growth in the prepared composites. The current research study presents the development of an improved hybrid biocomposite material that has potential in biomedical implants.

1. Introduction

A single matrix comprising of more than one filler, which are interacting at nanometer scale, forms a hybrid composite. Incorporation of maximum of two fillers is usually found more appropriate and beneficial when designing a hybrid system, as it seems to give superior impact strength, balanced tensile strength, good thermal stability, enhanced dielectric properties, biocompatible properties, and improved miscibility between the components in the composite [1]. The concept of ternary composites over binary composites has been introduced to develop materials having improved interfacial interaction between the components that make them, hence imparting a greater control over the final system. The addition of sisal fiber in coconut sheath fiber-reinforced composites forms a hybrid composite shows a reduction in free holes as well as voids too [2]. Since, ternary composites promote enhanced impact strength, they are mainly focused on load bearing applications, especially in automobile industry, telecom applications, food packaging sector, and medical implants [3–5]. Thermoplastic matrix-based hybrid composites are taking over the present scenario, especially as bone implant materials. The commercially available bone implant materials such as HAPEX ™ and MEDPOR (porous high-density polyethylene [HDPE]) generally consist of polyethylenes as matrix. HDPE has been used as implants as MEDPOR (1985) in the field of maxillofacial defects as it can easily become stable against bones and could integrate with the bone tissues [6,7]. The minimal soft tissue reaction, ability to shape depending upon the nature of the bone and stability makes them a good choice in bone implant materials [8,9]. The main parameter in bone-implant interaction is the porosity that promotes rapid bone and fibrous ingrowth into the implant [10]. This could be achieved by employing fillers and additives in the system. It has been reported that, HDPE-chitosan composites have exhibited a maximum tensile strength of 19.7 MPa [11]. At the same time, the presence of

* Corresponding author.
E-mail address: francistania76@gmail.com (T. Francis).

https://doi.org/10.1016/j.mtsust.2022.100186
2589-2347/

plasticizers and compatibilizers improves the microstructural interaction and segmental mobility of a composite system, providing improvement in the mechanical properties of the system. Maleic anhydride has been used as compatibilizers for various thermoplastic based bio-composites due to its improved miscibility and better mechanical strength achieved by the system [12]. Natural vegetable oils especially palm oil, canola oil and olive oil have been replacing most petroleum based plasticizers for the development of polymer based biomaterials. The presence of the olefinic group in vegetable oils helps them to easily interact with the polymeric chains. Among them, palm oil is considered as an attractive renewable plasticizer, which can mix homogeneously with polyethylenes. Furthermore, the OH groups and C=C groups of palm oil can be utilized in tuning the properties of the developed composite systems. Studies shows that acrylated palm olein has been incorporated in systems for drug carriers, bio-polymeric scaffold material, bone implant materials etc. [13,14]. The presence of 5 wt% crude palm oil in HDPE and low-density polyethylene have shown a small reduction in impact strength but have promoted orientation strengthening in the composites. Hence, palm oil as plasticizer can be promoted for tough plastic materials for providing flexibility to the system and providing more interfacial interaction [15].

The most commonly used filler in medical implant is nano-hydroxyapatite, a chemical compound having the structural properties similar to the inorganic component of the bone. HAPEX ™ (60% HDPE and 40% hydroxyapatite) is used worldwide as bone substitute material. The mechanical strength of HAPEX ™ has been reported as 20.85 ± 30 MPa [16]. HDPE-HA composites have been improved by employing silane modification and the tensile strength has been increased to 23.16 ± 0.40 MPa [17]. It has also been noticed that the HDPE-hydroxyapatite system have limited applications due to increased brittleness. Composites based on polylactic acid (PLA)- hydroxyapatite were also prepared to improve the stiffness of the system. The system has achieved an impact strength of 32 kJ/m^2 [18]. Modifications based on hydroxyapatite-chitosan systems have also been studied widely for bone tissue engineering applications. Chitosan is obtained from deacetylated chitin, which is a natural polymer found in the exoskeleton of crustaceans. It is structurally similar to glycosaminoglycan, a major component in bone responsible for modulating the bone precursor cells for bone regeneration, which can promote cell growth in the prepared implant [19]. More hydrophilic or more hydrophobic surface has a negative impact on cell proliferation. A neutral condition where the contact angle lies in between 70 and 90° is considered appropriate for protein absorption and cell adhesion. The wettability of the system can be altered with the concentration and presence of the filler that is reinforced. This further explains why hybrid systems like ternary composites are capable of neutral wettability and good cell proliferation. Until now, various binary composites and ternary composites consisting of thermoplastic polymers such as HDPE, low-density polyethylene, ultrahigh molecular weight polyethylene-based biocomposites have been developed for bone implant materials with good cell viability. Here, the present study is focusing on the modification of the commercially available bone implant materials by converting it into a ternary system by adding chitosan to HDPE-hydroxyapatite system (HAPEX ™). The biocompatibility of palm oil-based systems has not been studied until now, and hence, the present work investigates the biocompatibility and microstructural analysis of plasticized HDPE-chitosan composite systems and HDPE–chitosan–hydroxyapatite composites for the first time.

The present work is focusing on the modification of commercially available thermoplastic polyethylene implants by introducing a natural polymer–chitosan and an inorganic mineral–hydroxyapatite as fillers to form a hybrid composite system. The aim of the work was also to improve the mechanical strength and nontoxicity of the samples. Furthermore, the bonding and interaction between the newly added components to the existing polyethylene were studied using microstructural analysis techniques such as PALS, XRD, and FTIR. The activation energy data obtained from thermogravimetric analysis (TGA) experiment have been used to analyze the thermal stability of the system. The surface properties of the system were analyzed and have been correlated with water contact angle measurements and cell proliferation studies.

2. Experimental

2.1. Materials and methodology

HDPE (density: 0.950 gm/cm^3) was provided from Reliance Industries Limited, India, and low molecular weight chitosan (degree of deacetylation (DD) > 85%) was received as gift from Kerala State Cooperative Federation for Fisheries Development Ltd (Matsyafed), Kerala, India. Palm oil used as plasticizer was procured from Parisons Pvt. Ltd. KINFRA Park, Kozhikode, India. Hydroxyapatite (<200 nm), dicumyl peroxide, and maleic anhydride were of analytical grade and were obtained from Sigma-Aldrich (India).

2.2. Preparation of HDPE–chitosan–hydroxyapatite composites

Prior to mixing, chitosan and hydroxyapatite used as fillers were vacuum dried at 80 °C overnight to reduce the moisture content. Initially, HDPE–chitosan composites plasticized with 5 wt% of palm oil were prepared and optimized as reported in our previous studies [20]. The optimized HDPE–chitosan composite plasticized with palm oil has been used for the preparation of the ternary composite comprising of HDPE–chitosan–hydroxyapatite system. HDPE was initially melted at 160 °C and was mixed for 4 min; 5 wt% of chitosan and 5 wt% of palm oil were added to the melted HDPE and were again mixed for another 3 min. To the resulting system, varying concentration of hydroxyapatite was added for the development of the ternary composite. Dicumyl peroxide (0.5 wt%) and maleic anhydride (2 wt%) were added as free radical initiator and compatibilizer, respectively. The overall processing time was limited to 20 min. The synthesized composite mixes shown in Table 1 were hydraulic pressed and then injection molded for further characterizations.

2.3. Characterizations

2.3.1. Fourier transform infrared analysis

The attenuated total reflectance-Fourier transform infrared (ATR–FTIR) spectrometric analysis using Thermo Fischer Scientific, Nicolet iS5 was used to study the interaction between HDPE, chitosan, and hydroxyapatite in the composite system. A small section

Table 1
Formulation of HDPE–chitosan and HDPE–chitosans–hydroxyapatite composites.

Sample	HDPE (g)	Chitosan (wt%)	Hydroxyapatite (wt%)	Palm oil (wt%)
HC0	30	–	–	–
HC5	30	5	–	–
HP5	30	5	–	5
HA1	30	5	2	5
HA2	30	5	4	5
HA3	30	5	6	5
HA4	30	5	8	5
HA5	30	5	10	5

of the pressed sample was scanned from 4000 cm^{-1} to 400 cm^{-1} range with 32 scans for each sample.

2.3.2. X-ray diffractometry (XRD)

The XRD analysis was carried out with Rigaku Miniflex 600 (5th gen) employing Cu-Kα radiation (λ = 1.5405 Å) and Ni filter at an operating voltage of 40 kV and 15 mA. The relative intensities were recorded within 5–80 (2θ) range at a scanning rate of 0.5°/min.

2.3.3. Thermogravimetric analysis (TGA)

TGA has been employed to study the thermal stability and activation energy of the polymeric composites prepared. The study was carried out using TG/DTA, STA7200 (Hitachi) at a heating rate of 10 °C/min from 30 to 1000 °C, with 6–7 mg of the sample in platinum pans in a nitrogen environment. The rate of nitrogen gas was maintained at 100 ml/min during the experiment. Ultrasensitive microbalance noted the weight changes throughout the experiment. Weight loss versus temperature and time was recorded online using Measure software. The activation energy analysis was conducted using Coats Redfern Model to study the thermal stability of the material.

2.3.4. Impact strength analysis

The Izod impact strength (un-notched) of the rectangular samples was found by using Resil Impactor Junior (CEAST) (ASTM D256). The specimens were tested on the impact tester having 4J capacity and striking velocity of 3.6 m/s. The specimen held as vertical cantilevered beam is broken by a pendulum. The impact resistance is obtained from the values directly read from the tester.

2.3.5. Positron annihilation lifetime spectroscopy (PALS)

Free hole volume studies for HDPE–chitosan–hydroxyapatite composites were studied using a positron annihilation lifetime spectrometer as reported by Ravikumar et al. [21]. PATFIT-88 is used in combination with a proper source to apply background correction on the obtained reproducible spectra. Three Gaussian time resolution functions facilitate a better pattern of the positron lifetime spectra for the prepared composites.

2.3.6. Contact angle measurements

Contact angle measurements were conducted to study the wettability as well as hydrophilicity of the samples. They were conducted by sessile drop method using water at room temperature using Digidrop–MCAT goniometer (GBX).

2.3.7. Water sorption analysis

Water sorption of the composites were done as per ASTM D570-81. Initial weight of the dried samples were obtained. It was then submerged in distilled water at room temperature until constant weight was observed [22]. The excess water on the surface of the composite after soaking is removed carefully, and the weight of the composite was again weighed with a Mettler balance type having precision of 0.1 mg. The water absorption ability (%) is calculated as:

$$\text{sorption}(\%) = \left(\frac{W_n - W_d}{W_d}\right) * 100 \quad (1)$$

where, W_d is the original dry weight of the sample and W_n is the weight of the composite after immersion. The test was carried out for triplicate samples, and the average value was taken for further calculations.

2.3.8. Cell proliferation studies

Proliferative efficacy of the test compounds was studied using Methyl Thiazolyl Tetrazolium (MTT) assay. Mouse osteoblast cells (MC3T3) were cultured in minimal essential medium with alpha modifications (alpha-MEM) supplemented with 10% FBS, 1% antibiotic-antimycotic solution, and 1% L-glutamine. Cells were maintained at 37 °C and 5% CO_2 in a humidified atmosphere. The assessment of cell proliferative efficacy was conducted by seeding the cells onto the test films in 96 well microtiter plates at a seeding density of 5000 cells/well; 24 h after incubation with test materials, the MTT reagent was added to the wells and incubated at 37 °C for 4 h. Formazan crystals were solubilized using DMSO, and absorbance was recorded at 570 nm using multimode microplate reader (FluoSTAR Omega, BMG Labtech). Percentage proliferation of the cells was calculated with respect to untreated cell control. Photomicrographs of the cells treated with different test materials were captured using an axiocam attached to an inverted microscope (PrimoVert, Cerl Zeiss).

3. Results and discussion

3.1. Fourier transform infrared spectroscopy (FTIR)

The interaction of HDPE with hydroxyapatite and chitosan studied using FTIR are presented in Fig. 1 and Scheme 1 respectively. The interaction of palm oil plasticized HDPE-chitosan composites was reported in detail in our previous studies [20]. In the spectra given below, the C–*O*–C asymmetric stretching of bridge oxygen of chitosan normally found at 1151 cm^{-1} is shifted to 1129 $cm^{-1}$when incorporated into the HDPE matrix. The peak at 1712 cm^{-1} is slightly shifted to 1719 $cm^{-1}$with the addition of palm oil to HDPE–chitosan system. The peak broadening observed in HDPE-CS composites has also disappeared on addition of palm oil [12,22]. The characteristic peaks around 1050, 571, and 561 cm^{-1} corresponding to the different modes of PO_4 groups in hydroxyapatite are observed in HA4 composite system [23]. When hydroxyapatite is added to HP5, the intensity of peaks at 2915 and 2844 cm^{-1} is decreased notably. Broadening of peaks under the region of 1200 and 1000 cm^{-1} helps identify the formation of interlinked bonds between the phosphate bonds of hydroxyapatite and C–O or C–H bonds of chitosan [24]. The restriction of molecular vibrations by PO_4^{3-} ions of hydroxyapatite could be ascribed to the broadening of peaks at 1050 cm^{-1} [23,25,26]. Scheme 1 presents the possible interactions between the components HDPE, chitosan, and hydroxyapatite.

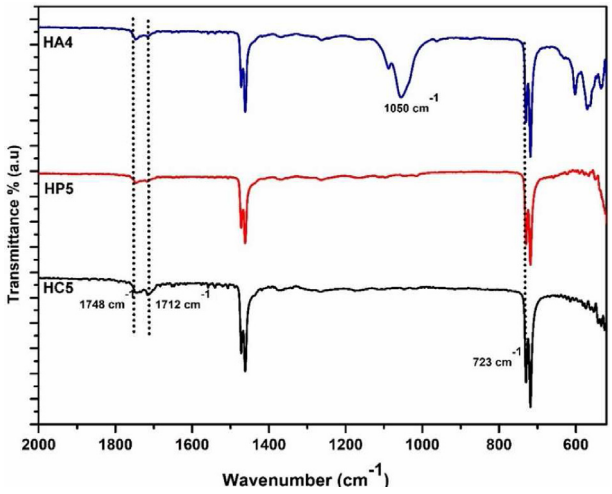

Fig. 1. FTIR spectra of HC5, HP5, and HA4.

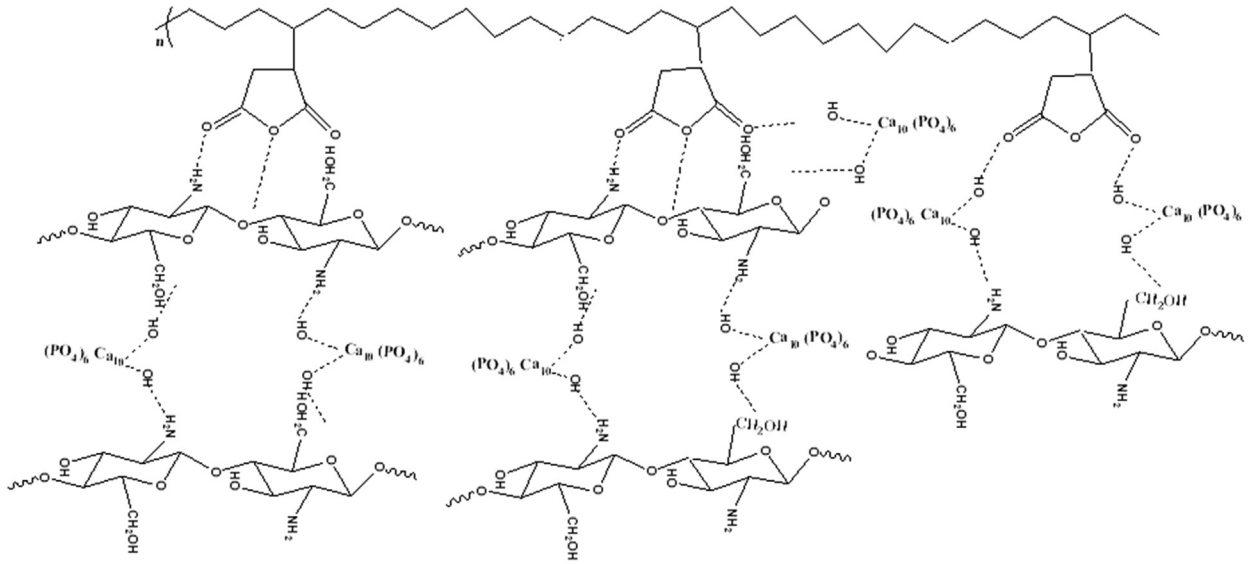

Scheme 1. Possible interaction of chitosan and hydroxyapatite with compatibilized HDPE.

3.2. X-ray diffractometry (XRD)

The XRD spectra of the developed composites are displayed in Fig. 2. The peaks at 2θ = 21.4°, 2θ = 23.8°, and 2θ = 36.27° scattering from (110), (200), and (020) planes indicate the orthorhombic structure of polyethylene (ICDD # 53–1859). The characteristic peak of chitosan at 2θ = 20° is found overlapped by HDPE, as observed in all graphs. The slight decrease in peak intensity for HP2 was noted which can be due to the difference in size of the chitosan particles incorporated and the lattice strain developed in the system [26]. The hydroxyapatite-added ternary system has peaks at 2θ = 25.8°, 31.7°, 32.16°, and 32.8° corresponding to the diffraction from (002), (221), (222), and (060) (ICDD # 05–0656). Absence of significant changes for the main orientation planes of HDPE, chitosan, and hydroxyapatite indicates no phase separation, making it suitable for maintaining the biological properties of the prepared composites [27,28].

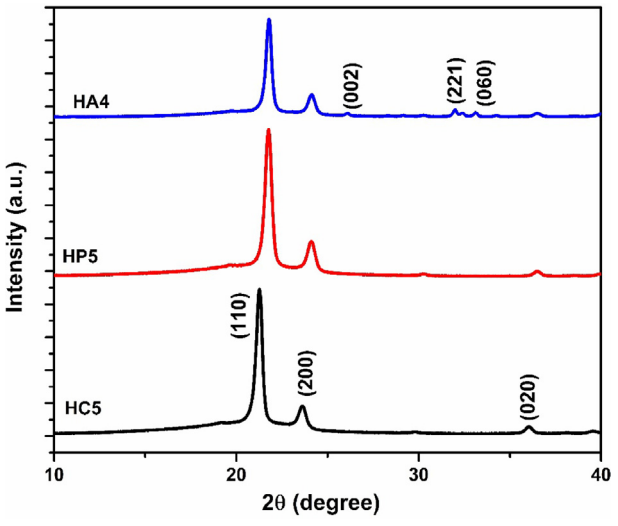

Fig. 2. XRD spectra of HC5, HP5, and HA4.

3.3. Thermogravimetric analysis (TGA)

The thermal behavior of HC0, HDPE–chitosan, and HDPE–chitosan–hydroxyapatite composites shown in Fig. 3 was evaluated to study the thermal stability of the prepared composites as well as to employ them in sterilization process when considered as bio-implants [29]. The degradation process of HDPE-chitosan-hydroxyapatite composites was found to be similar to the HDPE–chitosan systems [30]. Apart from the one-step degradation (between 400 and 600 °C) of HC0 corresponding to the thermolytic rupture of the macromolecular polymer units, the addition of chitosan and hydroxyapatite had gone through a major degradation in the range of 230–420 °C and 420–500 °C. A slight degradation noted in the region of 90–160 °C is attributed to the evaporation of water trapped by the hydrophilic OH groups of chitosan in the composite system. This change is negligible in HA4 system, indicating the compatibility of chitosan with HDPE and hydroxyapatite. The commencement of degradation for HA4 is starting at 428 °C showing good miscibility between hydroxyapatite and plasticized HDPE–chitosan system. The highest degradation temperature and lowest % weight loss as observed from the graphs also support the strong interface compatibility between hydroxyapatite and the composite system. The inorganic component has undergone no phase change throughout the TG analysis. The degradation temperature has also increased gradually with the addition of hydroxyapatite and is nearing to that of HP5.

The influence of fillers on the thermal stability is further supported through the activation energy analysis obtained from Coats–Redfern's method. By adopting first-order linear rate for the process and by combining the Arrhenius equation, the Coats–Redfern Model is obtained as [30]:

$$\ln\left(\frac{-ln(1-\alpha)}{T^2}\right) = \ln\left(\frac{AR}{\beta E}\right)\frac{-E}{RT} \quad (2)$$

A = pre-exponential factor (min^{-1}), E = activation energy($Jmol^{-1}$), and β = heating rate ($Kmin^{-1}$). The kinetic parameters were obtained from TG/DTG analysis. By plotting $\ln\left(\frac{-ln(1-\alpha)}{T^2}\right)$ vs $\frac{1}{T}$, a straight line with slope $\frac{E}{R}$ and intercept $\ln\left(\frac{AR}{\beta E}\right)$ is obtained. The calculation of activation energy using Coats–Redfern equation for

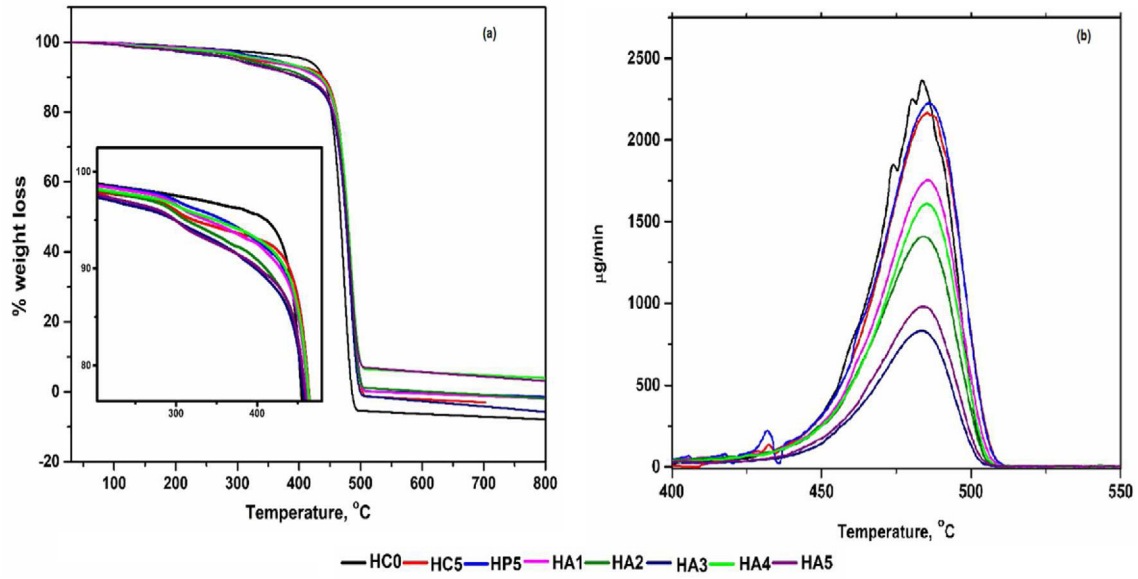

Fig. 3. **(a)** TGA and **(b)** DTG analysis of HDPE−chitosan−hydroxyapatite composites.

HDPE−chitosan−hydroxyapatite composites is shown in Table 2. HA4 exhibits highest thermal stability as evidenced by activation energy value of 333.2 kJ/mol among the HDPE−chitosan−hydroxyapatite composite systems. Further, the thermal stability increases gradually till HA4 and then decreases with higher concentration of hydroxyapatite. The addition of 10 wt% of hydroxyapatite has evidenced a decrease in the stability of the system, which could be attributed to the formation of agglomeration of hydroxyapatite in the system beyond the optimum concentration. The thermal decomposition of the composite has also been decreased with HA5, indicating the incompatibility between the components in the system.

3.4. Impact strength analysis

The impact strength analysis was conducted to evaluate the strength of the prepared HDPE−chitosan composites and HDPE−-chitosan−hydroxyapatite composites. Fig. 4 shows the impact strength of HC5, HP5, and HA(n) composites. An impact strength of 96 ± 3 kJ/m^2 was obtained for HC0, which was higher than non-compatibilized HDPE [31]. The addition of 5 wt% of chitosan to HC0 caused an increase in impact strength to105 ± 2 kJ/m^2. This increase could be attributed to the good interfacial bonding between the reactive groups of chitosan with compatibilized HDPE [32]. Meanwhile, the addition of 5 wt% of palm oil as plasticizer reduced its strength to 102 ± 2 kJ/m^2. A slightly lower yet a similar impact strength of HP5 with HC5 can be ascribed to the same way in which the matrix deforms to impact tests, indicating the formation of a stronger interface [33,34]. Furthermore, the long alkyl chains of palm oil help in easier relaxation of polymer chains in the composite. Hence, the impact energy could disperse more quickly into the composite system [35]. When varying concentration of hydroxyapatite was added to HP5, impact strength is initially reduced to 98 ± 2 kJ/m^2. With the addition of 8 wt% of hydroxyapatite, the impact strength increased. This increase could be ascribed to two main reasons: (a) the interaction of more flexible amino group of chitosan with the stiff and polar groups of hydroxyapatite. This reduces the flexibility of the HDPE/CS/HA system and (b) ability of the composite to hold the impact energy due to minimum number of microcracks formed in the system, due to good filler−matrix interaction [36,37]. Beyond 8 wt% of hydroxyapatite, the impact strength is reduced to 88 ± 2 kJ/m^2, indicating agglomeration formed in the system imparting more brittle nature to the composite.

Table 2
Activation energy analysis and degradation behavior of HDPE−chitosan−hydro xyapatite composite.

Sample	Initial degradation (°C)	Final degradation (°C)	E_a (kJmol^{-1})	R
HC0	394	506	324.7	0.9923
HC5	434	511	348.0	0.9997
HP5	429	512	348.2	0.9998
HA1	416	508	331.11	0.9948
HA2	417	509	308.4	0.9961
HA3	418	505	92.07	0.9632
HA4	428	509	333.2	0.9907
HA5	423	505	226.3	0.9714

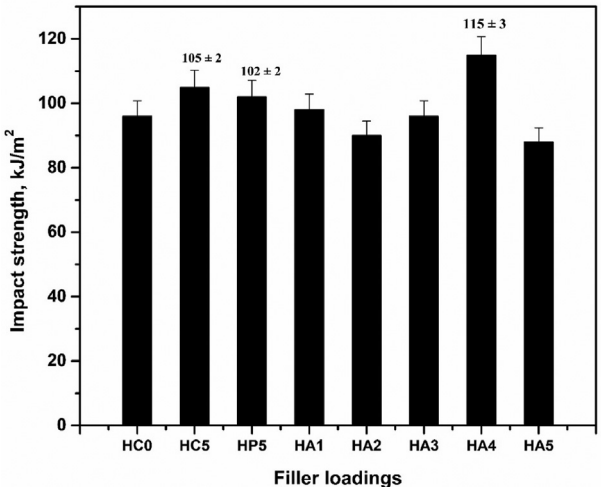

Fig. 4. Impact strength of HDPE−chitosan−hydroxyapatite systems.

Table 3
PALS data of HDPE–chitosan–hydroxyapatite composites.

Sample Code	τ_3(ns) ±0.010	I_3±0.16	V_f (Å)3±0.96	F_V±0.003
HC0	2.15	16.30	111.96	0.127
HC5	2.06	16.55	103.21	0.118
HP5	1.90	25.63	88.25	0.157
HA1	1.89	26.63	87.39	0.161
HA2	2.05	21.92	102.26	0.156
HA3	1.90	27.03	88.49	0.166
HA4	2.19	15.92	115.82	0.128
HA5	2.11	15.26	108.07	0.114

3.5. Positron annihilation lifetime spectroscopy (PALS)

The effect of varying concentration of hydroxyapatite on HDPE/chitosan system on the free hole volume of the composite is given in Table 3. The o-Ps lifetime (τ_3) depends on the size of free holes, whose intensity (I_3) is found to be proportional to the fraction of free hole volume holes (F_v). The miscibility of HDPE with chitosan and hydroxyapatite is clearly noted from the voids and holes formed. This affects the crosslinking properties and crystallinity. The addition of varying concentration of fillers affects the crosslinking properties, which further affects the size of free volume holes formed in the composite. From the results, it is observed that τ_3 increases till HA4 when increasing concentration of hydroxyapatite is added and then shows a decrease at HA5. When nanosized fillers are added into a polymer matrix, chain mobility of macromolecules in the tightly bound layers on the surface of the filler decrease. This affects the size of free volume hole formed in the system.

Miscibility and phase separation seem to have a stronger effect on the fractional free volume of the composite. The decrease of I_3 can also be related not only toward the inhibition of positronium formation but also due to the extent of miscibility obtained through enhanced crosslinking and filler addition. The values of I_3 are quite close in all composites with slight variations at lower concentration of hydroxyapatite. With the increase in the concentration of hydroxyapatite, more molecules are involved in the formation of effective interaction between HDPE–chitosan and hydroxyapatite [38]. The reactive groups of chitosan interacting with HDPE/chitosan composites suppress the formation of free volume holes at higher filler concentration. Beyond the optimized composition of HA4, small hydroxyapatite particles could fill the free holes in the composite. This might be the cause of low free hole volume in HA5 [39]. The results are better supported by the low impact strength in HA5 than HA4. τ_3 is found to be lower in HA1, but changes non-linearly with the addition of filler. Beyond a certain limit, apart from the breaking of certain interactions, hydrogen bonding takes place between the polar groups of crosslinked HDPE/chitosan and hydroxyapatite. This leads to the consequent separation of chitosan chains, making it available for interaction with hydroxyapatite. The incorporation of filler content brings at higher concentration produces large number of pores with smaller size. But, in composites below 8 wt% of hydroxyapatite addition, pores with bigger sizes are prominent which is reflected from the results [40]. The incorporation of hydroxyapatite also increases the grafting ratio in the composites. The more voluminous group increases the surface area of the composites, and hence, volume fraction increases [41].

3.6. Water sorption studies and water contact angle measurements

The physical characteristics of the composite such as surface roughness and aggregation of filler in the matrix decide the biocompatibility of a material. As reported in previous studies, neat HDPE and chitosan had contact angle values at 101° and 85°, respectively. The values of HDPE–chitosan systems and HDPE–-chitosan–hydroxyapatite systems had values lying in between 50° and 85° making them appropriate for cell adhesion and protein absorption. The hydrophilic value of HC0 at 78.9° ± 2 can be attributed to the reactive anhydride groups on HDPE. When

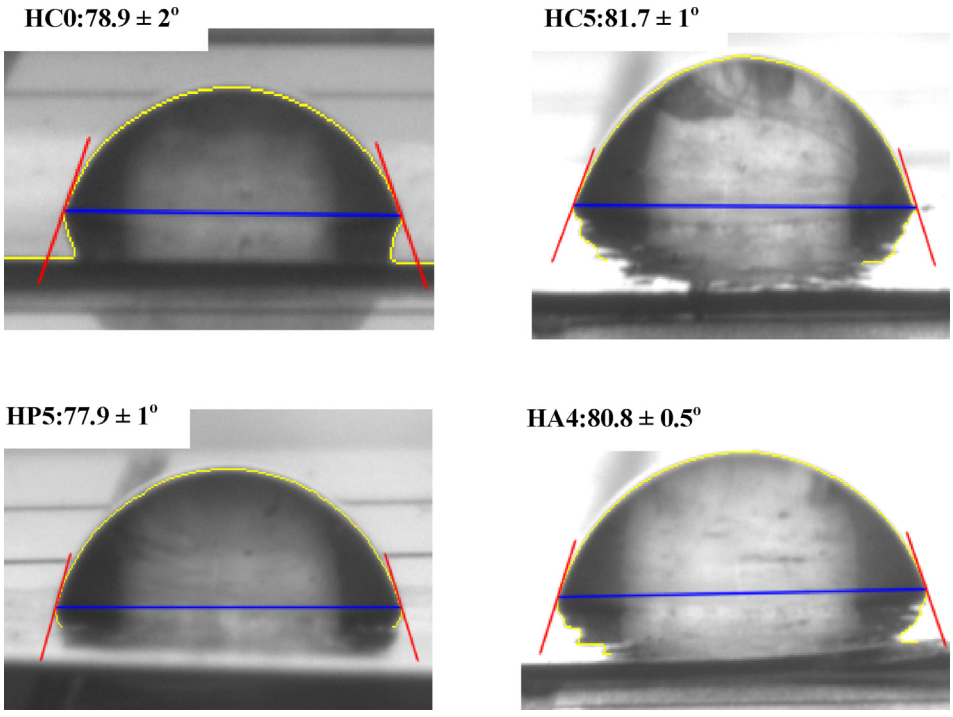

Fig. 5. Contact angle images of the prepared composites.

chitosan is added to HC0, the hydrophilicity of the composite is reduced slightly. This can be ascribed to the surface alterations at the microscale which have a profound effect on the contact angle properties [42,43]. When hydroxyapatite is added, the contact angle is further changed to 80.8°. This can be ascribed to the more amorphous nature attained by the composite on addition of hydroxyapatite which attains the capability of absorbing water and further restricts the spreading of water on the film surface. Contact angle images of the composites are given in Fig. 5.

The percentage of water sorption for HDPE–chitosan composites and HDPE–chitosan–hydroxyapatite composites is given in Fig. 6. An increased water uptake is observed in all composites in the initial 10 days. This decreases slowly in the following days. HDPE–chitosan systems show more sorption characteristics than HDPE–chitosan–hydroxyapatite composites. The less availability of the reactive functional groups, arising due to the interaction between chitosan and compatibilized HDPE could be attributed to the high sorption rate in HC5 and HP5 as observed from the graphs. When palm oil is added to HC5, the segmental mobility within the composite provides more space within it. This results in more water uptake [44]. The plasticizer has the ability to increase segmental mobility thereby increasing the free hole volume of the composite, so that the system can adsorb more water. This can further promote water clustering at successively higher hydration levels [45]. The presence of hydroxyapatite has significantly reduced the water sorption rate as observed in the previous reports. The water sorption ability of HA4 has increased over time, making it suitable for bone implant material. When water is sorbed at a higher rate, the polymer chains can undergo a relaxation process such that the probability of elution of unreacted monomer chains trapped in the composite matrix becomes more easier. This can contribute to the degradation of the implant–bone bonds over time, which has been reported in various studies [46].

3.7. Cell proliferation studies

The in-vitro cell proliferative behavior on the composites was evaluated using MC3T3-E1 mouse osteoblast cells. This property assessed by MTT assay after 24 h of exposure to the test materials. The percentage of proliferation of the cells was calculated with respect to the untreated cell control, as shown in Table 4. The cell proliferation level on plasticized HC5 and HA4 was higher than HC0. This enhancement may be due to the presence of nano-hydroxyapatite in the composites, which boosted the osteoblastic phenotype to be effectively proliferated. The cell proliferation was observed to be very low in HC5 and also in the unplasticized HDPE–chitosan–hydroxyapatite composite system. The addition of palm oil to HC5 and HA4 certainly increased the crosslinking and interaction between the components in the composite system. The relative decrease in cell proliferation in HC5 and HP5 can be attributed to the surface roughness of the composites. Increased surface roughness can retard cell proliferation, as reported by several studies. Grit blasting and hydrophobic character of the diamond films were found to be responsible for the decrease in cell proliferation of hFOB human osteoblastic cell line [47]. Increase in the surface roughness decreased the cell proliferation and migration of MG63 osteoblast-like cells via decreased expression of angiogenic and osteogenic markers [48]. The composites with low surface roughness are known to increase the cell proliferation of human osteoblast-like cells significantly due to its effects on calcium nodule formation and alkaline phosphatase activity enhancement [49]. Similar results were obtained in the present study. The composites possessed mechanical properties similar to the natural bone and promoted cell proliferation. Use of chitosan phosphate in polymeric matrix ensured the uniform distribution of the particles along with particle–polymer interfacial interactions and promoted proliferation of L929 mouse fibroblasts [50]. Higher mechanical strength of the polymer composites provides significant support for enhanced shelf-life in the *in vivo* scenario for biomedical and tissue regenerative applications. Biomaterials with compressive and elastic strength are known to be comparable to the host tissue promoting structural integrity for clinical applications [51]. Enhancement of the mechanical strength remains a challenge in bone tissue engineering [52]. Prepared polymeric composites displayed increased mechanical strength indicating its promising future utilization in biomedical applications.

The cell proliferation and cell distribution were assessed via phase-contrast microscopy is shown in Fig. 7. It is also noted that the highly proliferated pre-osteoblasts had small globules of mineral deposits on them together with better cellular attachments. As observed, the palm oil-added samples enhanced cell proliferation. Cell density was found to be highest in HP5 followed by HA4, HC0, and HC5, respectively. Compared to the untreated control cells, the spherical and elongated shaped cells adhered to the polymeric composite films displayed higher proliferation, as indicated by the compact distribution of circular/elongated shaped cells. All the tested composites showed good cytocompatibility on osteoblasts and hence can be promising for biomedical applications after further pre-clinical and clinical validation.

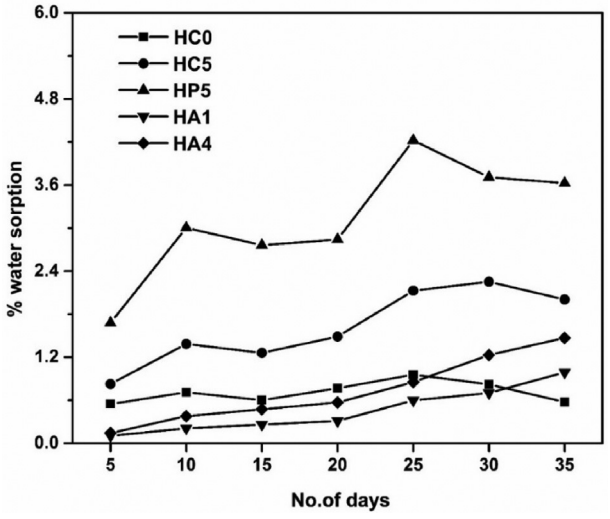

Fig. 6. Sorption studies of the prepared composites.

Table 4
Proliferative efficacy of the test materials on MC3T3 E1 cells assessed using MTT assay.

Sample code	Cell proliferation (Mean% ± SD)
HC0	118.13 ± 3.33
HC5	104.53 ± 3.03
HP5	142.67 ± 3.61
HA4	125.87 ± 5.33

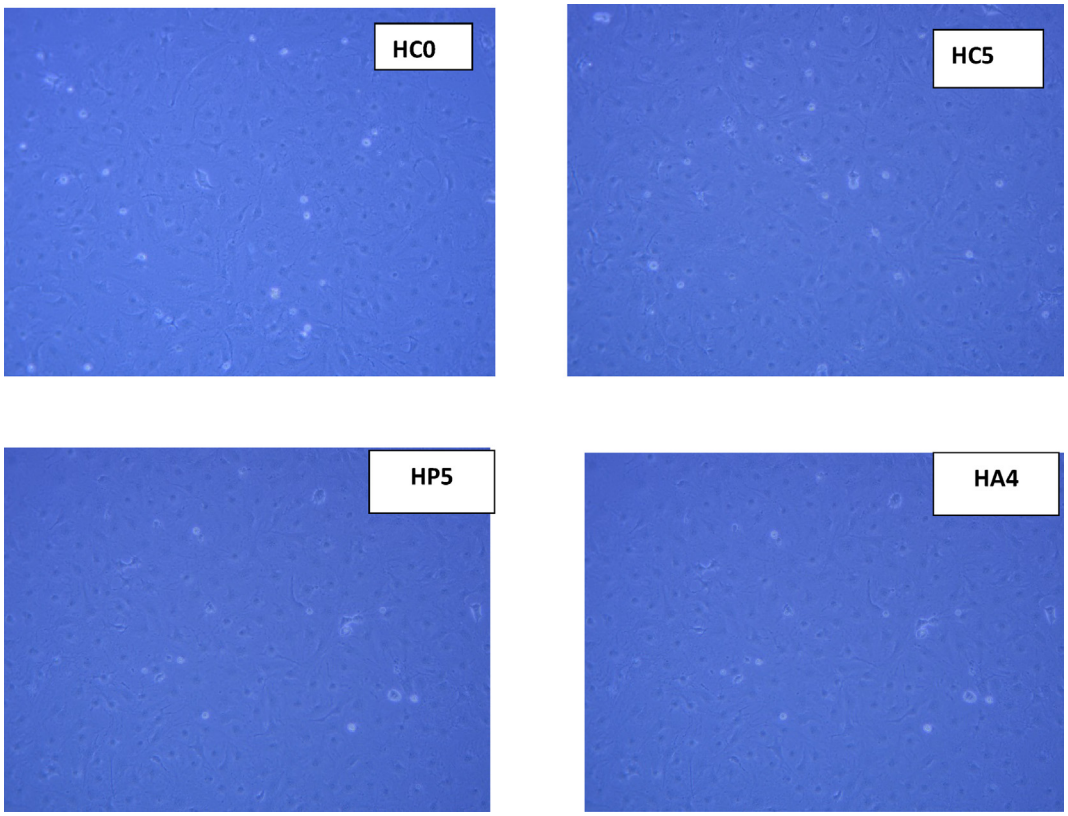

Fig. 7. Fluorescence images obtained during cell studies.

4. Conclusions

The thermal, structural, and mechanical analysis of a binary composite (HDPE−chitosan) and ternary composite (HDPE−chitosan−hydroxyapatite) is compared and analyzed. The structural analysis using XRD and FTIR shows no phase separation between the fillers and matrix. The HDPE−chitosan composite with 5 wt% palm oil (HP5) has been optimized due to its good miscibility of the components in the system and enhanced thermal stability. Furthermore, the addition of 8 wt% of hydroxyapatite to HP5 showed improved stability and enhanced mechanical performance. The impact strength of HA4 has been increased by 12% than its corresponding binary system HP5. Phase change variations were not observed during TGA analysis, which further supports the XRD analysis. Higher activation energy of HA4 at 333 kJ/mol shows the miscibility of hydroxyapatite with chitosan. The forming of large number of pores with reduced pore size makes the prepared system suitable for increased osteointegration as observed from the biocompatibility analysis. Contact angle measurements were obtained in the range of 70 to 85° making them suitable for cell adhesion. The biocompatible studies using MC3T3 E1 cell analysis also showed good biocompatibility with fibroid like structures formed on the system for the optimized systems. The results support that chitosan and hydroxyapatite incorporated HDPE system can be considered as a classical implant material with improved energy absorbing ability when subjected to an external impact force and biocompatible nature which can further be recommended for clinical research. The increased use of day petroleum-based porous HDPE implants could be substituted with an effective implant with better mechanical performance which comprises of HDPE as matrix and chitosan and hydroxyapatite as fillers for a variety of applications with the aim of reducing the amount of petroleum-based products.

Credit author statement

Category 1

Conception and design of study: Meril Shelly, Tania Francis.

Acquisition of data: Meril Shelly, Raghavendra M, Ashwini Prabhu, H.B. Ravikumar.

Analysis and/or interpretation of data: Meril Shelly, Ashwini Prabhu, H.B. Ravikumar, Meril Mathew, Tania Francis.

Category 2

Drafting the manuscript: Meril Shelly, Tania Francis.

Revising the manuscript critically for important intellectual content: Meril Shelly, Ashwini Prabhu, H.B. Ravikumar, Meril Mathew, Tania Francis.

Category 3

Approval of the version of the manuscript to be published: Meril Shelly, Raghavendra M, Ashwini Prabhu, H.B. Ravikumar, Tania Francis.

Declaration of competing interest

The authors declare that they have no known competing financial interests or personal relationships that could have appeared to influence the work reported in this paper.

Acknowledgments

The authors like to acknowledge Kerala State Council for Science, Technology and Environment (KSCSTE) and Rashtriya Uchchatar Shiksha Abhiyan (RUSA) for the financial support.

References

[1] S. Banerjee, B.V. Sankar, Mechanical properties of hybrid composites using finite element method based micromechanics, Compos. B Eng. 58 (2014) 318−327, https://doi.org/10.1016/j.compositesb.2013.10.065.

[2] M. Chandrasekar, K. Senthilkumar, T.S.M. Kumar, I. Siva, P.S. Venkatanarayanan, M. Phuthotham, N. Rajini, S. Siengchin, M.R. Ishak, Effect of Adding Sisal Fiber on the Sliding Wear Behavior of the Coconut Sheath Fiber-Reinforced Composite, Tribology of Polymer Composites: Characterization, Properties, and Applications, Elsevier, Amsterdam, Netherlands, 2021, pp. 115–125.
[3] G.S. Sailaja, S. Velayudhan, M.C. Sunny, K. Sreenivasan, H.K. Varma, P. Ramesh, Hydroxyapatite filled chitosan-polyacrylic acid polyelectrolyte complexes, J. Mater. Sci. 38 (2003) 3653–3662, https://doi.org/10.1023/A:1025689701309.
[4] M.N. Gururaja, A.H. Rao, A review on recent applications and future prospectus of hybrid composites, Int. J. Soft Comput. 1 (2012) 352–355.
[5] R. Ranjan, A. Kumar, S. Kumar, K. Badiyani, Role of high density porous polyethylene (H.D.P.E) implants in correction of maxillofacial defects and deformity: a review, Int. J. Prev. Clin. Dent. Res. 2 (2015) 71–75.
[6] M. Khorasani, P. Janbaz, F. Rayati, Maxillofacial reconstruction with Medpor porous polyethylene implant: a case series study, J. Korean Assoc. Oral Maxillofac. Surg. 44 (2018) 128–135, https://doi.org/10.5125/jkaoms.2018.44.3.128.
[7] M. Ziąbka, E. Menaszek, J. Tarasiuk, S. Wroński, Biocompatible nanocomposite implant with silver nanoparticles for otology—in vivo evaluation, Nanomaterials 8 (2018) 764, https://doi.org/10.3390/nano8100764.
[8] J.L. Frodel, S. Lee, The use of high-density polyethylene implants in facial deformities, Arch. Otolaryngol. Head Neck Surg. 124 (1998) 1219–1223, https://doi.org/10.1001/archotol.124.11.1219.
[9] S. Deshpande, A. Munoli, Long-term results of high-density porous polyethylene implants in facial skeletal augmentation: an Indian perspective, Indian J. Plast. Surg. 43 (2010) 34–39, https://doi.org/10.4103/0970-0358.63955.
[10] J. Liang, R. Wang, R. Chen, The impact of cross-linking mode on the physical and antimicrobial properties of a chitosan/bacterial cellulose composite, Polymers 11 (2019) 491, https://doi.org/10.3390/polym11030491.
[11] M. Di Maro, M.G. Faga, G. Malucelli, F.D. Mussano, T. Genova, R.E. Morsi, A. Hamdy, D. Duraccio, Influence of chitosan on the mechanical and biological properties of HDPE for biomedical applications, Polym. Test. 91 (2020) 106610, https://doi.org/10.1016/j.polymertesting.2020.106610.
[12] M. Sunilkumar, T. Francis, E.T. Thachil, A. Sujith, Low density polyethylene–chitosan composites: a study based on biodegradation, Chem. Eng. J. 204 (2012) 114–124, https://doi.org/10.1016/j.cej.2012.07.058.
[13] R. Tajau, R. Rohani, M.S. Alias, N.H. Mudri, K.A. Abdul Halim, M.H. Harun, N. Mat Isa, R. Che Ismail, S. Muhammad Faisal, M. Talib, M. Rawi Mohamed Zin, Emergence of polymeric material utilising sustainable radiation curable palm oil-based products for advanced technology applications, Polymers 13 (2021) 1865, https://doi.org/10.3390/polym13111865.
[14] W.N.F.M. Zulkifli, Bioplasticiser and Palm Oil. Corpus ID: 52999318, 2019.
[15] C.T. Ratnam, A.M. Min, T.G. Chuah, A.R. Suraya, T.S. Choong, W.W. Hasamuddin, Physical properties of polyethylene modified with crude palm oil, Polym. Plast. Technol. Eng. 45 (2006) 917–922, https://doi.org/10.1080/03602550600723563.
[16] M. Wang, R. Joseph, W. Bonfield, Hydroxyapatite-polyethylene composites for bone substitution: effects of ceramic particle size and morphology, Biomaterials 19 (1998) 2357–2366, https://doi.org/10.1016/S0142-9612(98)00154-9.
[17] S. Deb, M. Wang, K.E. Tanner, W. Bonfield, Hydroxyapatite-polyethylene composites: effect of grafting and surface treatment of hydroxyapatite, J. Mater. Sci. Mater. Med. 7 (1996) 191–193, https://doi.org/10.1007/BF00119729.
[18] J.O. Akindoyo, M.D. Beg, S. Ghazali, H.P. Heim, M. Feldmann, Imspact modified PLA-hydroxyapatite composites–Thermo-mechanical properties, Compos. - A: Appl. Sci. Manuf. 107 (2018) 326–333, https://doi.org/10.1016/j.compositesa.2018.01.017.
[19] C.D.G. Abueva, B.T. Lee, Poly(vinylphosphonic acid) immobilized on chitosan: a glycosaminoglycan-inspired matrix for bone regeneration, Int. J. Biol. Macromol. 64 (2014) 294–301, https://doi.org/10.1016/j.ijbiomac.2013.12.018.
[20] M. Shelly, M. Raghavendra, H.B. Ravikumar, T. Francis, Structural and free-hole volume characterization of high-density polyethylene-chitosan composites plasticized with palm oil, Polym. Eng. Sci. 1, 2021, https://doi.org/10.1002/pen.25818.
[21] H.B. Ravikumar, C. Ranganathaiah, Compatibilizer-induced microstructural changes in poly(trimethylene terephthalate)/EPDM blends studied by the positron annihilation lifetime technique and differential scanning calorimetry, Polym. Int. 54 (2005) 1288, https://doi.org/10.1002/pi.1845.
[22] K.R. Mohamed, H.H. Beherei, Z.M. El-Rashidy, In vitro study of nano-hydroxyapatite/chitosan–gelatin composites for bio-applications, J. Adv. Res. 5 (2014) 201–208, https://doi.org/10.1016/j.jare.2013.02.004.
[23] H. Fouad, R. Elleithy, O.Y. Alothman, Thermo-mechanical, wear and fracture behavior of high-density polyethylene/hydroxyapatite nano composite for biomedical applications: effect of accelerated ageing, J. Mater. Sci. Technol. 29 (2013) 573–581, https://doi.org/10.1016/j.jmst.2013.03.020.
[24] D.B. Dreghici, B. Butoi, D. Predoi, S.L. Iconaru, O. Stoican, A. Groza, Chitosan–hydroxyapatite composite layers generated in radio frequency magnetron sputtering discharge: from plasma to structural and morphological analysis of layers, Polymers 12 (2020) 3065, https://doi.org/10.3390/polym12123065.
[25] F. Heidari, M.E. Bahrololoom, D. Vashaee, L. Tayebi, In situ preparation of iron oxide nanoparticles in natural hydroxyapatite/chitosan matrix for bone tissue engineering application, Ceram. Int. 41 (2015) 3094–3100, https://doi.org/10.1016/j.ceramint.2014.10.153.
[26] S.H. Kim, B.K. Lim, F. Sun, K. Koh, S.C. Ryu, H.S. Kim, J. Lee, Preparation of high flexible composite film of hydroxyapatite and chitosan, Polym. Bull. 62 (2009) 111, https://doi.org/10.1007/s00289-008-1008-5.
[27] K. Agrawal, G. Singh, D. Puri, S. Prakash, Synthesis and characterization of hydroxyapatite powder by sol-gel method for biomedical application, J. Miner. Mater. Charact. Eng. 10 (2011), 727-734.10.4236/jmmce.2011.108057.
[28] Y. Li, T. Liu, J. Zheng, X. Xu, Glutaraldehyde-crosslinked chitosan/hydroxyapatite bone repair scaffold and its application as drug carrier for icariin, J. Appl. Polym. Sci. 130 (2013) 1539–1547, https://doi.org/10.1002/app.39339.
[29] M. Shakir, R. Jolly, M.S. Khan, N. e Iram, H.M. Khan, Nano-hydroxyapatite/chitosan–starch nanocomposite as a novel bone construct: synthesis and in vitro studies, Int. J. Biol. Macromol. 80 (2015) 282–292, https://doi.org/10.1016/j.ijbiomac.2015.05.009.
[30] M. Shelly, M. Mathew, P.P. Pradyumnan, T. Francis, Dielectric and thermal stability studies on high density polyethylene – chitosan composites plasticized with palm oil, Mater. Today Proc. 46 (2021) 2742–2746, https://doi.org/10.1016/j.matpr.2021.02.479.
[31] P.S. Lima, R. Trocolli, R.M. Wellen, L. Rojo, M.A. Lopez-Manchado, M.V. Fook, S.M. Silva, HDPE/chitosan composites modified with PE-g-MA. thermal, morphological and antibacterial analysis, Polymers 11 (2019) 1559, https://doi.org/10.3390/polym11101559.
[32] F.A. Tanjung, S. Husseinsyah, K. Hussin, Chitosan-filled polypropylene composites: the effect of filler loading and organosolv lignin on mechanical, morphological and thermal properties, Fibers Polym. 15 (2014) 800–808, https://doi.org/10.1007/s12221-014-0800-0.
[33] J. Xu, J.M. Eagan, S.S. Kim, S. Pan, B. Lee, K. Klimovica, K. Jin, T.W. Lin, M.J. Howard, C.J. Ellison, A.M. LaPointe, Compatibilization of isotactic polypropylene (*i*PP) and high-density polyethylene (HDPE) with *i*PP–PE multiblock copolymers, Macromolecules 51 (2018) 8585–8596, https://doi.org/10.1021/acs.macromol.8b01907.
[34] W. Wang, X. Zhang, Z. Mao, W. Zhao, Effects of gamma radiation on the impact strength of polypropylene (PP)/high density polyethylene (HDPE) blends, Results Phys. 12 (2019) 2169–2174, https://doi.org/10.1016/j.rinp.2019.02.020.
[35] S. Yu, W.M. Yek, S.Y. Ho, S.A. Rannou, S.H. Lim, Microstructure and impact strength of polyamide 6 composites, Mater, Today Commun 4 (2015) 199–203, https://doi.org/10.1016/j.mtcomm.2015.08.004.
[36] M. Yadav, K.Y. Rhee, S.J. Park, D. Hui, Mechanical properties of Fe_3O_4/GO/chitosan composites, Compos. B Eng. 66 (2014) 89–96, https://doi.org/10.1016/j.compositesb.2014.04.034.
[37] P.A. Sreekumar, N. Leblanc, J.M. Saiter, Effect of glycerol on the properties of 100% biodegradable thermoplastic based on wheat flour, J. Polym. Environ. 21 (2013) 388–394, https://doi.org/10.1007/s10924-012-0497-3.
[38] Y.Q. Wang, Y.P. Wu, H.F. Zhang, L.Q. Zhang, B. Wang, Z.F. Wang, Free volume of montmorillonite/styrene-butadiene rubber nanocomposites estimated by positron annihilation lifetime spectroscopy, Macromol. Rapid Commun. 25 (2004) 1973–1978, https://doi.org/10.1002/marc.200400380.
[39] M. Joshi, B.S. Butola, G. Simon, N. Kukaleva, Rheological and viscoelastic behavior of HDPE/octamethyl-POSS nanocomposites, Macromolecules 39 (2006) 1839–1849, https://doi.org/10.1021/ma051357w.
[40] Z.F. Wang, B. Wang, N. Qi, H.F. Zhang, L.Q. Zhang, Influence of fillers on free volume and gas barrier properties in styrene-butadiene rubber studied by positrons, Polymer 46 (2005) 719–724, https://doi.org/10.1016/J.POLYMER.2004.12.002.
[41] A. Pablo, M. Carlos, A. Javier, S. Alberto, A microstructural study of acrylic-modified chitosan by means of PALS and SAXS, Defect Diffus. Forum 373 (2016) 265–268, https://doi.org/10.4028/www.scientific.net/DDF.373.265.
[42] D. Kubies, L. Himmlová, T. Riedel, E. Chánová, K. Balík, M. Douderova, J. Bártová, V.J.P.R. Pesakova, The interaction of osteoblasts with bone-implant materials: 1. The effect of physicochemical surface properties of implant materials, Physiol. Res. 60 (2011) 95, https://doi.org/10.33549/physiolres.931882.
[43] S. Tamburaci, B. Cecen, O. Ustun, B.U. Ergur, H. Havitcioglu, F. Tihminlioglu, Production and characterization of a novel bilayer nanocomposite scaffold composed of chitosan/Si-nHap and zein/POSS structures for osteochondral tissue regeneration, ACS Appl. Bio Mater. 2 (2019) 1440–1455, https://doi.org/10.1021/acsabm.8b00700.
[44] M.L. Sanyang, S.M. Sapuan, M. Jawaid, M.R. Ishak, J. Sahari, Effect of plasticizer type and concentration on dynamic mechanical properties of sugar palm starch–based films, Int. J. Polym. 20 (2015) 627–636, https://doi.org/10.1080/1023666X.2015.1054107.
[45] M.A. Haq, F.A. Jafri, A. Hasnain, Effects of plasticizers on sorption and optical properties of gum cordia based edible film, J. Food Sci. Technol. 53 (2016) 2606–2613, https://doi.org/10.1007/s13197-016-2227-7.
[46] I.F. Ghazi, J.K. Oleiwi, S.I. Salih, M.A. Mutar, Water sorption and solubility of light-cured dental composites prepared from two different types of matrix monomers, in: IOP Conf. Ser.: Mater. Sci. Eng., vol. 1094, 2021, p. 12169.
[47] G. Heinrich, T. Grögler, S.M. Rosiwal, R.F. Singer, Validation of three-dimensional surface characterizing methods: scanning electron microscopy and confocal laser scanning microscopy, Surf. Coat. 94 (1997) 514–520, https://doi.org/10.1002/sca.4950230401, https://doi.org/10.1088/1757-899X/1094/1/012169.
[48] O. Andrukhov, R. Huber, B. Shi, S. Berner, X. Rausch-Fan, A. Moritz, N.D. Spencer, A. Schedle, Proliferation, behavior, and differentiation of

osteoblasts on surfaces of different microroughness, Dent. Mater. 32 (2016) 1374–1384, https://doi.org/10.1016/j.dental.2016.08.217.
[49] Y. Deng, X. Liu, A. Xu, L. Wang, Z. Luo, Y. Zheng, F. Deng, J. Wei, Z. Tang, S. Wei, Effect of surface roughness on osteogenesis in vitro and Osseo integration in vivo of carbon fiber-reinforced polyetheretherketone–nanohydroxyapatite composite, Int. J. Nanomedicine 10 (2015) 1425, https://doi.org/10.2147/IJN.S75557.
[50] N. Pramanik, D. Mishra, I. Banerjee, T.K. Maiti, P. Bhargava, P. Pramanik, Chemical synthesis, characterization, and biocompatibility study of hydroxyapatite/chitosan phosphate nanocomposite for bone tissue engineering applications, Int. J. Biomater. (2009) 1–8, https://doi.org/10.1155/2009/512417.
[51] G. Turnbull, J. Clarke, F. Picard, P. Riches, L. Jia, F. Han, B. Li, W. Shu, 3D bioactive composite scaffolds for bone tissue engineering, Bioact. Mater. 3 (2018) 278–314, https://doi.org/10.1016/j.bioactmat.2017.10.001.
[52] J. Venkatesan, S.K. Kim, Chitosan composites for bone tissue engineering—an overview, Mar. Drugs 8 (2010) 2252–2266, https://doi.org/10.3390/md8082252.